CO adsorption on Pt-induced Ge nanowires

Danny E. P. Vanpoucke* and Geert Brocks
Computational Materials Science, Faculty of Science and Technology and MESA+ Institute for Nanotechnology, University of Twente, P.O. Box 217, 7500 AE Enschede, The Netherlands

(Received 8 February 2010; revised manuscript received 4 June 2010; published 28 June 2010)

Using density-functional theory, we investigate the possible adsorption sites of CO molecules on the recently discovered Pt-induced Ge nanowires (NWs) on Ge(001). Calculated scanning tunneling microscope (STM) images are compared to experimental STM images to identify the experimentally observed adsorption sites. The CO molecules are found to adsorb preferably onto the Pt atoms between the Ge nanowire dimer segments. This adsorption site places the CO molecule in between two nanowire dimers, pushing them outward along the NW direction, blocking the nearest equivalent adsorption sites. This explains the observed long-range repulsive interaction between CO molecules on these Pt-induced nanowires.

DOI: 10.1103/PhysRevB.81.235434 PACS number(s): 68.43.Bc, 73.20.Hb, 68.37.Ef

I. INTRODUCTION

In the last several decades, CO adsorption on Pt surfaces has been studied extensively both experimentally and theoretically. This large interest is partly due to the deceiving simplicity of the system and its industrial importance in catalytic processes, such as CO oxidation and Fischer-Tropsch synthesis.[1,2]

However, a simple system such as CO adsorbed on the Pt(111) surface, has and still does cause quite some controversy. Three decades ago, adsorption site preference and measured adsorption energies were the subject of discussion among experimental researchers. These problems have meanwhile been resolved and experimental results have converged to a coherent and detailed picture of this system.[3–7] On the theorists side however, a discussion has emerged during the last decade regarding the unexpected failure of prevalent density-functional theory (DFT) approximations to properly predict the CO/Pt(111) site preference. From experiment it is found that the on-top site is most stable in the low-density regime while local density approximation (LDA) and generalized gradient approximation (GGA) calculations show a preference for the threefold coordinated hollow adsorption site. The cause of this CO/Pt(111) puzzle seems to originate from the tendency of LDA and GGA to favor higher coordination and the flatness of the potential surface describing adsorption of CO on the Pt(111) surface.[8] This has lead to a search for better or alternative functionals in recent years.[9,10]

Although the incorrect site prediction is a problem for DFT, this does not mean that the obtained geometries and derived physical properties are incorrect.[11] Even more, the calculated scanning tunneling microscope (STM) images derived from the geometries show excellent qualitative agreement with the experiment.[12,13]

With the recent discovery of Pt-induced nanowire (NW) arrays on Ge(001), a new Pt-based adsorption surface becomes available.[14] Decoration of these NWs with CO molecules opens the way to the formation of one-dimensional (1D) molecular chains. Although the adsorption of single CO molecules on these Pt-induced NWs has been observed experimentally, true molecular chains remain to be observed.[15,16]

The first room-temperature (RT) STM experiments, by Öncel *et al.*,[15] showed the CO molecules to be very mobile along the NWs. Later, Kockmann *et al.*[16] performed experiments at 70 K to suppress this mobility and observed a long-range repulsive interaction between pairs of CO molecules on the same NW. In those experiments the NWs were considered to be composed of Pt dimers in the troughs of a modified Ge(001) surface, called β terrace,[14] allowing for a straightforward interpretation of the observed STM images. The CO molecules were suggested to be adsorbed on the bridge positions of the NW dimers, comparable to the adsorption of CO on the Pt(001) surface.[15,16] Calculations on the interaction of CO with a free standing Pt monatomic wire suggest a similar behavior.[17]

However, in recent theoretical studies we showed the NWs to be modeled by Pt induced Ge NWs.[18,19] In this model, contrary to the experimentally assumed model, the NWs consist of Ge dimers placed in the Pt lined troughs of a Pt modified Ge(001) reconstructed surface. Because the sticking probability and affinity for CO on Ge is known to be low,[20] while being high for Pt, it would be surprising if CO molecules would adsorb on the NW itself. This leads to the suggestion that the theoretical models, proposed in Refs. 18 and 19, are in disagreement with the experiment, even though their calculated STM images show very good agreement with the experimental STM images of the NWs. To investigate this apparent disagreement we study the adsorption of CO molecules on Pt-induced NWs, starting from our previously proposed theoretical models for the NWs.[18,19,21] Using *ab initio* DFT calculations, formation and adsorption energies are calculated. Theoretical STM images, generated using the Tersoff-Hamann method, are compared to experimental STM images to identify the adsorption sites and geometries observed in experiment, reconciling the theoretical models with the experimental observations.

This paper is structured as follows: In Sec. II the used theoretical methods are described. In Sec. III we present our results, which will be discussed more in depth in Sec. IV. Finally, in Sec. V the conclusions are given.

II. THEORETICAL METHOD

The calculations are performed within the DFT framework using the projector augmented waves method and the

Ceperley-Alder LDA functional, as implemented in the VASP program.[22–25] A 400 eV kinetic-energy cutoff is applied for the plane-wave-basis set. CO molecules are placed on the models of both types of Pt-induced NWs on Ge(001) presented in Ref. 19. The surface/NW system is modeled by periodically repeated slabs of 12 layers of Ge atoms with NW reconstructions on both surfaces. A vacuum region of ~15.5 Å is used to separate the periodic images of the slab along the z axis. Due to the computational cost and the small size of the CO molecule a (2×4) surface cell, for the solitary wire geometry, and a (4×4) surface cell, for the array wire geometry, is used. The Brillouin zone of the 2×4 (4×4) surface unit cell is sampled using a 8×4 (4×4) Monkhorst-Pack special k-point mesh.[26] To optimize the geometry of the surface/adsorbate system the conjugate gradient method is used while the positions of the Ge atoms in the center two layers are kept fixed as to represent the bulk of the system.

STM images are calculated using the Tersoff-Hamann method in its most basic form with the STM tip approximated as a point source.[27] The integrated local density of states (LDOS) is calculated as $\bar{\rho}(\mathbf{r},\varepsilon)\propto\int_{\varepsilon}^{\varepsilon_F}\rho(\mathbf{r},\varepsilon')d\varepsilon'$ with ε_F the Fermi energy. Because the tunneling current is proportional to the integrated LDOS in the Tersoff-Hamann model, an STM tip following a surface of constant current can be simulated through plotting a surface of constant (theoretical) LDOS: $\bar{\rho}(x,y,z,\varepsilon)=C$ with C a constant. For each C this construction returns a height z as a function of the position (x,y). This height map is then mapped linearly onto a gray scale. The constant C is chosen such that the isosurface has a height z between 2 and 3 Å above the highest atom of the surface.

III. RESULTS

As was shown in previous work, a small difference exists between solitary NWs (NW1) and NWs in arrays (NW2).[28] In experiment this difference presents itself as the appearance of a (4×1) periodicity at lower temperatures, which was traced back to the presence of an extra Pt atom bound to every pair of NW dimers.[19,29] Since this extra Pt atom introduces new possible adsorption sites and geometries, CO adsorption on both NW geometries needs to be studied.

Because some of the initial adsorption geometries relaxed into the same final structure, and because in some cases the geometry was modified extensively during relaxation, the adsorption sites presented in this manuscript are those found after relaxation. The NW geometry is a metastable configuration and the adsorption of CO sometimes introduces large deformations of the surface. Therefore we define both a formation and adsorption energy in these systems. The formation energy E_f indicates the energy gain/loss of the entire system due to the CO adsorption and the subsequent changes in the surface structure. It is defined [per (4×2)-surface unit cell] as

$$E_f=(E_{\mathrm{NW+CO}}-E_{\mathrm{pristNW}}-N_{\mathrm{CO}}E_{\mathrm{CO}})/2 \quad (1)$$

with $E_{\mathrm{NW+CO}}$ the total energy of the adsorbate-surface system, E_{pristNW} the total energy of a pristine slab+NW system and E_{CO} the total energy of a free CO molecule. N_{CO} is the number of CO molecules per surface unit in the system and the division by two is because CO is adsorbed at both faces of the slab. A negative value of the formation energy E_f indicates an increase in stability of the system.

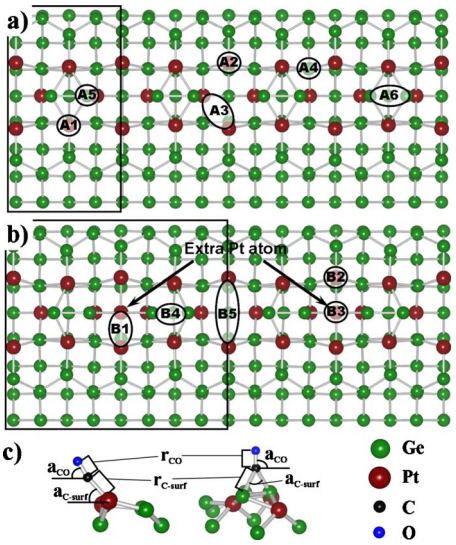

FIG. 1. (Color online) Adsorption sites of CO on (a) a solitary NW geometry and (b) an array NW geometry. Green (red) balls indicate the positions of the germanium (platinum) atoms. Black rectangles indicate surface unit cells. The circles indicate top adsorption sites while ellipses indicate bridge configurations with the binding surface atoms at the apexes of the ellipses. In case of the NW2 surface, the location of the extra Pt atom is indicated (Refs. 19 and 21). (c) Ball and stick representations of the two typical CO adsorption configurations: t(op) on the left and b(ridge) on the right. The bond lengths and angles discussed in the text and Tables I and III are indicated.

The adsorption energy E_{ad} refers to the binding energy of the CO molecule to the surface. Here any contribution due to surface deformation is excluded. It is defined (per CO molecule) as

$$E_{ad}=(E_{\mathrm{NW+CO}}-E_{\mathrm{NW+sd}}-N_{\mathrm{CO}}E_{\mathrm{CO}})/(2N_{\mathrm{CO}}) \quad (2)$$

with $E_{\mathrm{NW+sd}}$ the total energy of the surface with the adsorption-induced deformations but without adsorbed CO molecule.

A. CO on solitary NWs

Solitary NWs consist of Ge dimers located in the Pt lined troughs of a Pt-modified Ge(001) surface. We will refer to this structure as NW1. Figure 1(a) shows the adsorption sites (Ax) studied for the NW1 surface reconstruction. For the A3 adsorption site, two different configurations were found, shown in Fig. 2. In what follows we will use A3 to refer to both configurations, and A3a and A3b to refer to the specific ones. The A3 and A6 configurations show CO molecules in bridging geometries, with the C atom in a bridge configuration with two Pt or Ge atoms, respectively. All other A configurations shown in Fig. 1(a) are *top* configurations. The adsorption and formation energies are given in Table I, as are some geometrical parameters of the CO molecule adsorbed on the surface, defined in Fig. 1(c).

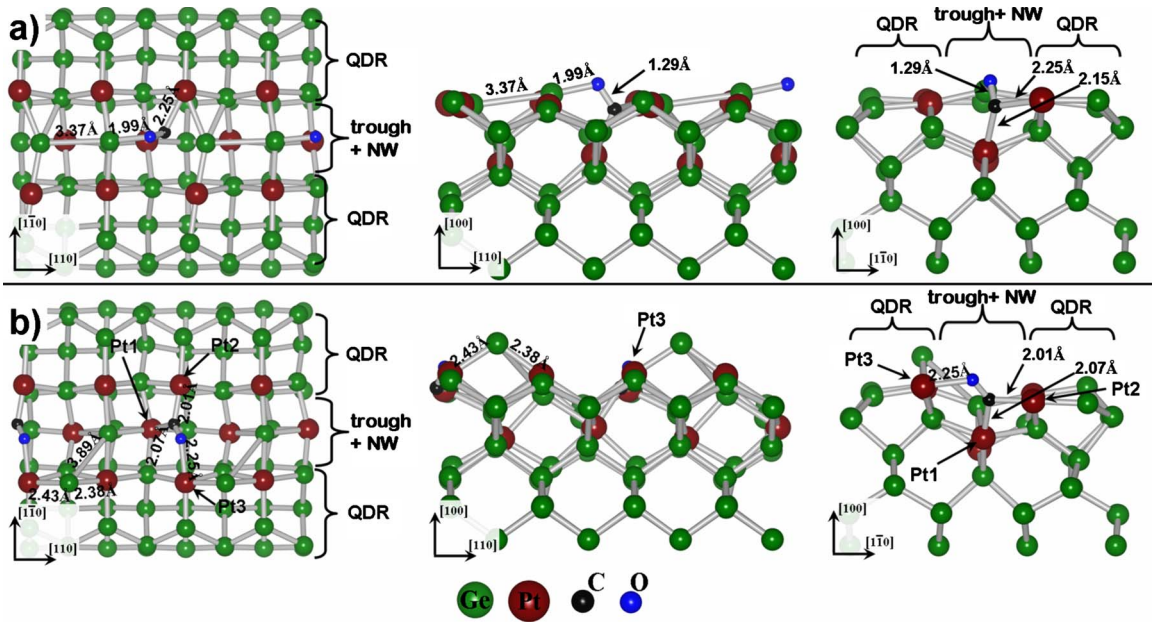

FIG. 2. (Color online) Ball-and-stick representations of the relaxed (a) A3a and (b) A3b adsorption structures: top view on the left, and side views parallel (center) and orthogonal (right) to the NW direction. The QDRs and troughs are indicated for the top view and the orthogonal side view. Bond lengths of interest are given. For the A3b configuration, the three atoms on which the CO molecule is adsorbed are indicated. Also note the Ge NW dimer atom ejected onto the QDR in the A3b configuration.

The dimer length $\mathbf{r}_{CO}$ of a free CO molecule was calculated to be 1.1330 Å, in good agreement with the experimental value.[30] Table I shows the CO bond lengths are only slightly stretched in most cases: about 1.59–1.85 %. The exception being CO adsorbed in the A3 configurations where the stretching is 13.95% and 7.15%. The difference between these last two configurations and the other configurations is the extra bond of the O atom with one of the surface atoms. In case of the A3a configuration the O atom has an extra bond with a Ge dimer atom [cf. Fig. 2(a)] while in the A3b configuration it is bound to a Pt atom of the top layer at the opposite side of the trough [cf. Fig. 2(b)]. Another interesting geometrical feature is that in most cases the adsorbed CO molecule is tilted with regard to the surface normal, unlike the behavior of CO molecules on clean Pt surfaces. In contrast, CO molecules adsorbed on top of Pt atoms, the C-Pt bond length is just slightly longer than what is found for CO on Pt(111) in an on-top configuration.[1,31]

The adsorption energies given in Table I show a very clear preference for CO adsorption on Pt (sites A1–A4). The values of E_{ad} might indicate that CO also binds weakly to the Ge NW atoms (sites A5 and A6), contrary to the experimental knowledge that CO does not bind to Ge. However, one needs to bear in mind that LDA tends to overbind, which in

TABLE I. Formation and adsorption energies for CO adsorbed on the NW1 surface. Adsorption sites are shown in Fig. 1(a). t (b) refers to top (bridge) adsorption. $\mathbf{r}_{CO}$ and $\mathbf{r}_{C\text{-surf}}$ are the C-O and C-Pt(Ge) bond lengths. For the A3 adsorption sites the value between brackets is the C-Pt bond length between C and the Pt atom in the bottom of the trough. $\mathbf{a}_{CO}$ and $\mathbf{a}_{C\text{-surf}}$ are the bond angles with regard to the surface plane. In case of bridge adsorption $\mathbf{a}_{C\text{-surf}}$ is the angle between the two C-surface bonds.

	E_f (eV)	E_{ad} (eV)	Coord. of C	$\mathbf{r}_{CO}$ (Å)	$\mathbf{a}_{CO}$ (deg)	$\mathbf{r}_{C\text{-surf}}$ (Å)	$\mathbf{a}_{C\text{-surf}}$ (deg)
			CO adsorbed on Pt atoms				
NW1 A1	−1.300	−1.747	t	1.152	88	1.906	86
NW1 A2	−1.721	−1.990	t	1.154	57	1.920	48
NW1 A3a	−1.156	−0.993	b	1.291	56	2.246 (2.150)	117
NW1 A3b	−1.485	−2.069	b	1.214	47	2.012 (2.066)	101
NW1 A4	−2.859	−1.890	t	1.152	63	1.907	62
			CO adsorbed on Ge NW atoms				
NW1 A5	−1.421	−0.439	t	1.151	70	2.015	70
NW1 A6	−0.349	−0.557	b	1.162	88	2.192	75

TABLE II. Adsorption and formation energies for the adsorption of one CO molecule per four NW dimers.

	A1	A2	A3b	A4	A5	A6
E_f (eV)	−3.60	−3.58	−5.56	−2.72	−0.78	−1.35
E_{ad} (eV)	−1.94	−2.11	−2.00	−1.94	−0.67	−0.39

this case results in the small adsorption energies. Furthermore, the binding energies of CO on Ge are $E_{ad} \cong 0.5$ eV while $E_{ad} \cong 2.0$ eV for CO adsorbed on Pt atoms, making the latter much more preferable, in agreement with the experimental expectations.

The A3 structures are a bit peculiar. Both have a bridge-like adsorption configuration and in addition the O atom also has a bond with a substrate atom [cf. Fig. 2]. Despite this similarity their adsorption energies differ more than 1.0 eV, making them the best and worst cases for CO adsorption on Pt atoms in this system. Furthermore, the least-stable A3a structure results in calculated STM images that show extremely good agreement with the experimental STM images obtained by Öncel *et al.*[15]

To understand why the A3a configuration is observed although appearing much less stable than the other A configurations on Pt, we have a look at the main contributions to the adsorption energy. The most important contribution in the A3a configuration comes from the CO bond stretching. To examine its effect, one can use a modified version of Eq. (2), replacing the formation energy of a relaxed gas molecule by the formation energy of a CO gas molecule with the same bond length as the adsorbed molecule. The resulting energy could then be considered the energy needed to desorb the molecule from the surface in a two step fashion. First, the bond(s) to the surface atoms are broken while the CO bond length remains unchanged. Then the molecule moves away from the surface relaxing to its equilibrium bond length. Since most adsorption geometries show only slightly stretched CO molecules, this energy only differs a little (~50 meV) from E_{ad}. However, for the strongly stretched A3 geometries a large difference with regard to E_{ad} is seen, resulting in energies of −2.010 eV and −2.384 eV for the A3a and A3b structures, respectively. This means that a CO molecule at an A3 site becomes the hardest to desorb from the surface using the path described above, explaining its observation by Öncel.

The complex adsorption geometry in case of the A3b site can be understood when it is compared to the adsorption of CO on a monatomic Pt wire. In their theoretical study, Sclauzero *et al.*[17] found that for an intermediate interplatinum distance of 3.7–5.3 Å a configuration with the CO molecule bridging the gap between two Pt atoms is the most stable configuration while for an interplatinum distance around 2.50 Å the bridge configuration, with the C atom bound to two Pt atoms, was found to be most favorable. In the A3b situation three Pt atoms are involved. Two (Pt1 and Pt2) are bound to the C atom and one (Pt3) is bound to the O atom. The distance between Pt1 and Pt2 is 3.145 Å while the distance between Pt1 and Pt3, and Pt2 and Pt3 is 3.958 and 5.008 Å, respectively. Both the latter values are in the intermediate range for the bridging configuration while the former value lies in the range where Sclauzero *et al.* found a simple bridge configuration to be most stable.

Returning to the energies, it follows from Eqs. (1) and (2) that the energy due to the surface deformation induced by the adsorption of a CO molecule is given by: $E_{sd}=E_f-E_{ad}$. Positive values of E_{sd} indicate a destabilization due to the adsorbed CO molecule (A1, A2, A3b, and A6) while negative values indicate a stabilization (A3a, A4, and A5). In Ref. 19 the NW1 geometry was shown to be a metastable configuration. It was also shown that the adsorption configuration with the Ge NW dimer bound to four surface dimers [site C in Fig. 11(a) in Ref. 19] has a more favorable formation energy than the NW1 structure [cf. Table III in Ref. 19, compare $\gamma^{\star}_{as}$ Ge NW A (NW1) to $\gamma^{\star}_{as}$ Ge NW C]. This explains the increased surface stability seen for CO adsorption sites A3a, A4, and A5. From the large differences between the adsorption and formation energies, it is expected that adsorption of CO on the NW1 system has a large influence on the geometry of the wire, as can be seen for example in Fig. 2. Because the range of the (destructive) influence of a CO molecule on the wire is larger than the size of the used surface cell, some calculations are carried out using a surface cell 4× the unit cell length. Only a single CO molecule is absorbed on it, effectively reducing the CO density by a factor of 4. Since the relaxation of such a huge cell is computational very demanding, lower accuracy relaxation parameters are used. E_f and E_{ad} are given in Table II showing even more clearly the effect of the CO molecule on the NW1 geometry

The large differences between E_f and E_{ad} again indicate large modifications of the NW1 structure. Comparing the relaxed geometries, we find that for larger differences between E_f and E_{ad}, more NW dimers are displaced or destroyed. In case of the A3b structure even all four NW dimers are somehow modified. This behavior might be the basis of the experimentally observed long-ranged repulsive interaction between CO molecules.[16] We will look into this aspect of CO adsorption in more detail in Sec. IV.

B. CO on NW arrays

In previous work it was shown that the NWs in NW arrays only differ very little from solitary NWs: a single extra Pt atom in the NW trough added to two NW1 unit cells, we will refer to this structure as NW2.[19,21] The extra Pt atom [indicated in Fig. 1(b)] binds to two NW dimers, inducing the observed 4×1 periodicity. This extra bond also stabilizes the NW. Through its construction, the unit cell of a NW2 surface is twice the size of that of the NW1 surface and since we only adsorb 1 CO molecule per surface, this effectively halves the CO coverage compared to that on the NW1 system.

TABLE III. Formation and adsorption energies for CO adsorbed on the NW2 surface. Adsorption sites are shown in Fig. 1(b). t (b) refers to top (bridge) adsorption. In case of the B5 adsorption site, the C atom is bound to only one Pt atom, however, the O is bound to the Pt atom at the opposite side of the trough resulting in the entire CO molecule forming a bridge. $\mathbf{r}_{CO}$ and $\mathbf{r}_{C\text{-surf}}$ are the C-O and C-Pt(Ge) bond lengths. $\mathbf{a}_{CO}$ and $\mathbf{a}_{C\text{-surf}}$ are the bond angles with regard to the surface plane. For the B1 adsorption site the value between brackets is the C-Pt bond length between C and the Pt atom at the bottom of the trough. For the B4 adsorption site the value between brackets is the C-Ge bond length to the Ge NW atom bound to the extra Pt atom in the trough. In case of bridge adsorption $\mathbf{a}_{C\text{-surf}}$ is the angle between the two C-surface bonds. Only for the B4 site the C atom is bound to Ge atoms, in all other cases the C atom is bound to a Pt atom in the surface.

	E_f (eV)	E_{ad} (eV)	Coord. of C	$\mathbf{r}_{CO}$ (Å)	$\mathbf{a}_{CO}$ (deg)	$\mathbf{r}_{C\text{-surf}}$ (Å)	$\mathbf{a}_{C\text{-surf}}$ (deg)
			CO adsorbed on Pt atoms				
NW2 B1	−1.424	−2.336	b	1.171	76	2.086 (2.004)	82
NW2 B2	−0.761	−1.911	t	1.154	77	1.911	74
NW2 B3	−1.033	−2.090	t	1.155	90	1.868	90
NW2 B5	−0.784	−2.197	t	1.170	20	1.883	28
			CO adsorbed on Ge NW atoms				
NW2 B4	−0.319	−0.916	b	1.163	62	2.003 (2.411)	72

Figure 2(b) shows the adsorption sites of CO on the NW2 4×4 surface cell after relaxation of the system.[32] Only the adsorption sites different from those already present in the NW1 geometry, i.e., those where the extra Pt atom is involved directly or indirectly, are investigated. Our observations for the adsorption sites on the NW1 surface are assumed also to be valid for the equivalent sites on the NW2 surface.

The adsorption energies per CO molecule and the formation energies per 4×2 surface cell are shown in Table III. Just as for the CO molecules adsorbed on Ge in the NW1 case, CO molecules adsorbed on Ge in the NW2 case (B4) have a much lower binding energy than CO molecules bound to Pt atoms, indicating the strong preference of CO toward Pt. The adsorption energies for CO molecules on Pt atoms are in the same range as for the NW1 system, albeit slightly higher on average. This might be due to the lower CO coverage in the NW2 systems, reducing the direct and indirect interaction between CO molecules. The on top A2 and B2 adsorption sites, on the NW1 and NW2 geometries, respectively, differ only by the presence of the extra Pt atom in the neighboring trough, resulting in comparable adsorption energies. However, the presence of the extra Pt atom in case of the NW2 system prevents the CO molecule of bending far toward the surface, increasing the angle $\mathbf{a}_{C\text{-surf}}$ from 48° to 74°.

On the other hand, in the B5 configuration, where no extra Pt atom is present nearby in the trough, the CO molecule bends further toward the surface and actually bridges the through connecting two Pt atoms at opposing sides of the trough. The distance between these Pt atoms is 4.826 Å, placing them in the regime where Sclauzero *et al.*[17] found a "*tilted bridge*" configuration to be the energetically preferred configuration.

In their study of CO adsorption on a freestanding monatomic Pt wire, Sclauzero *et al.* identified three regimes for the CO adsorption geometry. (i) For an unstretched (with Pt-Pt bond length $d_{Pt\text{-}Pt}=2.34$ Å) freestanding Pt wire, the bridge configuration was found to be favored with respect to the on-top configuration by about 1 eV. The energy of the bridge configuration was shown to have a minimum for a value for $d_{Pt\text{-}Pt}=2.50$ Å just slightly above the equilibrium Pt bond length of the chain. We will refer to this as the unstretched regime. (ii) In case of a hyperstretched configuration an energy minimum was found at $d_{Pt\text{-}Pt}=5.05$ Å. In this case the substitutional geometry was found to be more favorable than the bridge configuration. In the substitutional configuration the CO molecule is aligned parallel with the Pt wire, and the C and O atom are bound each to a half of the Pt wire. (iii) However, Sclauzero and his collaborators found the energy minimum of the substitutional geometry to be still slightly higher than the tilted bridge configuration. In this tilted bridge configuration the CO bond lies in a plane trough the wire but it is not aligned parallel or orthogonal to the wire. Although no energy minimum for this configuration was found, Sclauzero *et al.* found it to be preferred over the bridge and substitutional configuration for intermediate stretching lengths of the Pt-Pt distance (about 3.8 Å $\leq d_{Pt\text{-}Pt} \leq 5.1$ Å).

Although the monatomic wire studied by Sclauzero *et al.* is quite different from our current system, the interplatinum distances are comparable. Even more, in case of the NW2 geometry there are three Pt atoms (two on opposing sides of the trough and the extra Pt atom in the trough) forming a mini monatomic wire spanning the trough with three inequivalent adsorption sites located on it.

On this mini monatomic wire we find the adsorption site with the highest binding energy of all adsorption sites studied: the B1 site. For this adsorption site the CO molecule binds to two Pt atoms through a bridge configuration. The distance between the two Pt atoms is 2.682 Å, slightly longer than the optimum interplatinum distance for a CO molecule adsorbed in a bridge configuration on a monatomic freestanding Pt wire. Two other adsorption sites on the mini

monatomic wire are the B2 and B3 sites. These have an on-top configuration and are less favorable with adsorption energies 0.43 eV and 0.25 eV lower than the B1 site. This shows a nice qualitative agreement between this three-atom monatomic Pt wire present in the NW2 system and a free-standing monatomic Pt wire.

For all adsorption sites studied on the NW2 surface, the CO bond lengths are only stretched slightly, 1.85–3.35 %. Even more, comparing the values of $\mathbf{r}_{CO}$ and $\mathbf{r}_{C\text{-}surf}$ with those found by Sclauzero *et al.* shows perfect agreement for the CO bond length, and just fractionally larger lengths for the C-Pt distances in our embedded three-atom Pt wire. This slightly larger length is a simple consequence of the Pt atoms being embedded in the NW2 surface.

The B3 site is the only site where the CO molecule is perfectly perpendicular to the surface, this is due to the symmetry of the chemical environment. In contrast, the B2 adsorption site has a lower symmetry and the molecule bends along the asymmetry direction toward the three-atom monatomic Pt wire, i.e., toward the trough.

Contrary to CO adsorbed on the NW1 surface, CO adsorbed on the NW2 surface seems much less destructive. This is because the NW dimers are anchored at their position by the extra Pt atom. Only CO adsorbed at the B1 or B3 site modifies the NW significantly. In both cases, the CO molecule has a bond to the extra Pt atom, weakening the bonds with the NW dimers. Furthermore, in these configurations, the CO molecules are positioned between the NW dimers, pushing them outward, away from the molecule. The combination of these two effects is large enough to break the bonds between the NW dimers and the extra Pt atom. Because of the periodic boundary conditions and the size of our unit cell, the two NW dimers recombine to form a tetramer chain between the two copies of the CO molecule. In contrast to the NW1 surface, the free NW dimers will not be able to block the next equivalent adsorption site due to the presence of a NW dimer anchored in place by its accompanying extra Pt atom.

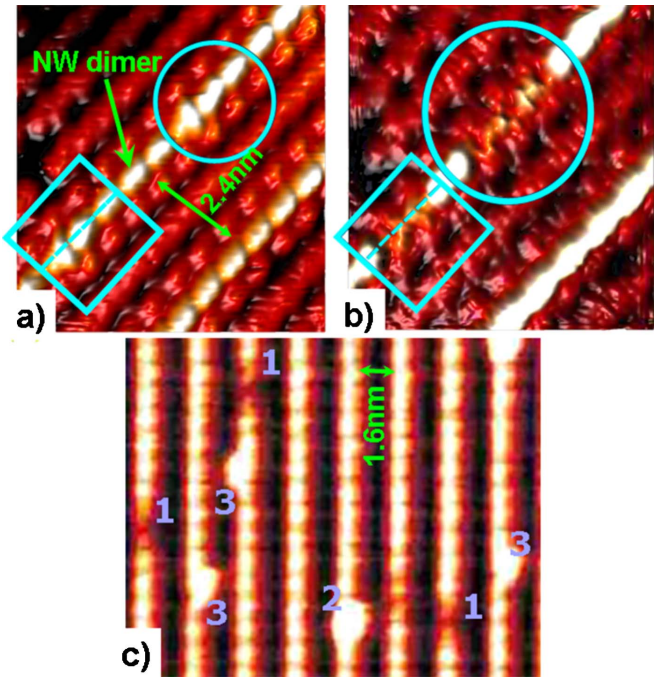

FIG. 3. (Color online) Experimental (a) filled- and (b) empty-state STM images of two CO molecules adsorbed on solitary nanowires. The used sample bias is −0.5 V for the filled state image and 0.2 V for the empty state image. In both cases a tunneling current of 0.44 nA is used. The circles and rectangles indicate the adsorption locations of the CO molecules. The dashed line in the rectangle gives the position of the line scan shown in Figs. 5(a) and 5(b). A single NW dimer is indicated in the filled state image, as is the distance between neighboring NWs. (c) Zoom out of a section of Fig. 1 in Ref. 16, an empty state STM image (+1.8 V; 0.5 nA) of CO-decorated NWs, recorded at 77 K. We have indicated three CO adsorption sites. Site 1 shows a large depression in the wire. Sites 2 and 3 show large protrusions. In case of site 2, the protrusion is centered on the NW while for site 3 the protrusion is centered either left or right of the NW. The NWs in the array are separated 1.6 nm.

IV. DISCUSSION

The results from the previous section show no clear-cut image for the CO-adsorption system based solely on calculated energies, which might already be suspected from the history of CO adsorption on pure Pt surfaces. However, direct comparison with experiment is possible by means of calculated STM images. This method has already been shown very successful at identifying correct adsorption sites for CO, even when the calculated energies fail to do so.[12,13] At the moment of writing only very little experimental work is available and the actual underlying NW type is not always entirely clear. The earliest experimental work on this system, by Öncel *et al.*,[15] presents the adsorption of CO molecules on NWs separated 2.4 Å, which based on our previous calculations (Ref. 19) leads to the assumption that these wires can be considered solitary NWs. In these experiments only one adsorption site was observed. It appears as a protrusion at negative bias and as a depression at positive bias. Later work, by Kockmann *et al.*,[16] studied the adsorption of CO molecules on arrays of NWs spaced only 1.6 Å. Based upon the results presented in Ref. 19, we assume these wires to have a NW2 geometry. Unlike Öncel *et al.*, Kockmann and collaborators observed two adsorption sites, both different from the one observed by Öncel *et al.* Based on this we will compare our results for solitary wires with the experiments of Öncel *et al.* and those for array NWs with the experiments of Kockmann *et al.*

A. CO adsorption on Pt-induced nanowires

As reference images for the experiment we will use the images given in Fig. 3. Figures 3(a) and 3(b) show CO adsorbed at solitary NWs, and Fig. 3(c) shows adsorption sites on the NW arrays.[15,16] Close examination of Fig. 3(c) shows three distinctly different adsorption sites, indicated 1, 2, and 3. Kockmann *et al.* on the contrary only identify two, considering sites 2 and 3 the same adsorption site. It is well known in literature that the electric field of an STM tip can influence the position and orientation of molecules adsorbed on a surface.[33] This can result in an extra broadening of the

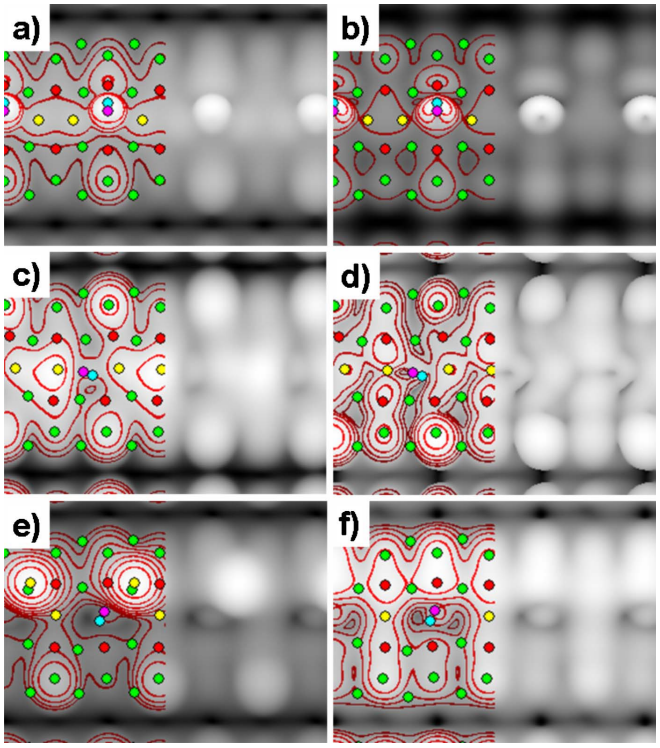

FIG. 4. (Color online) Calculated filled- and empty-state STM images for the A2 [filled (a) and empty (b)], A3a [filled (c) and empty (d)], A3b [filled (e)], and A3b1 [filled (f)] adsorption geometries. The simulated biases are for (a), (e), and (f) −1.50 V, (b) +1.50 V, (c) −0.70 V, and (d) +0.30 V. Contours are added to guide the eye, they are separated 0.3 Å. Colored disks indicate atomic positions: green and red represent Ge and Pt atom positions in the two top layers of the surface, yellow gives the position of the Ge atoms forming the NW, and cyan and fuchsia disks give the C and O positions.

CO image along the scan lines, which in this case is orthogonal to the NWs shown in Fig. 3(c). This, however, cannot cause the CO molecules at the adsorption site 2 to appear as site 3 since the latter is observed at both sides of the NW [cf. Fig. 3(c)].

In addition to the formation and adsorption energies, STM images are calculated for all NW1 and NW2 adsorption geometries. All NW1 CO adsorption geometries show protrusions for both positive and negative simulated bias with the exception of the A3a adsorption site. For the latter, a protrusion is visible in the filled state image [cf. Fig. 4(c)] while a depression is clearly present in the empty state image [cf. Fig. 4(d)]. The comparable A3b structure on the other hand shows a clear protrusion on the adjacent quasidimer row (QDR) for all biases [cf. Fig. 4(e)]. However, this protrusion is not caused by the CO-molecule present but by the Ge NW atom ejected from the trough instead [cf. Fig. 2(b)]. Removal of this Ge atom removes the protrusion and only a brightened Pt-Ge dimer, bound to the O atom, remains [cf. Fig. 4(f)]. The CO molecule itself remains invisible.

Of all adsorbed CO molecules only those on the A3 sites and on the Ge NW, are located "on" the NW. However, these are not the only CO molecules resulting in a CO image on the wire. Because of the large tilt angle of the CO molecule at the A2 site, the resulting image gives the impression of a CO molecule sitting, just slightly asymmetric, on top of the NW, as can be seen in Figs. 4(a) and 4(b). For large negative bias the image is round while becoming more and more bean shaped for smaller negative biases and all positive biases.

CO molecules bound to Ge NW atoms show images which look bean shaped for the on top adsorption site A5, and two-lobed donut shaped for the bridge adsorption site A6.

Based on the adsorption energies found in Sec. III, the adsorption of CO on the Ge NW dimers can be excluded. Only the Pt adsorption sites near the NWs remain. For the solitary NWs the A3b site can be excluded because for both positive and negative biases a depression is found, which is not reported in experiments.

The sites A1, A2, and A4 show a comparable behavior. Both in the filled and empty state pictures a large protrusion is clearly visible, slightly asymmetric to the NW position. This makes them possible candidates for the experimentally observed site 3 shown in Fig. 3(c). Figures 4(a) and 4(b) show an A2 adsorbed CO molecule as example.

The filled state picture of the A3a site shows a pear-shaped image for the NW dimer [cf. Fig. 4(c)] while the empty state picture shows no dimer image at all [cf. Fig. 4(d)]. Comparison of the experimental images observed by Öncel *et al.* [cf. Figs. 3(a) and 3(b)] show good agreement, despite the low adsorption energy calculated for this configuration.[15] However, as we showed in, taking the stretching of the CO molecule into account, this configuration becomes much more stable, explaining its observation in experiments.

Calculated line scans of the A3a adsorption site along the NW direction, with a line scan of a pristine NW as positional reference are shown in Fig. 5(c). The experimental line scans for the adsorption site observed by Öncel *et al.* are shown for comparison in Figs. 5(a) and 5(b).[34] Due to periodic boundary conditions and the fact that our unit cell contains only 1 NW dimer, this image can only be used to compare to the region $\sim 0.5 - \sim 1.5$ nm in Figs. 5(a) and 5(b). Note that the line scans in Figs. 5(a) and 5(c) are mirror images of each other (mirrored around the center of a NW dimer), indicating that the CO molecule was bound (the O-Ge bond) to the "left" side of the NW dimer in experiment while it is bound to the right side in our calculations, as is indicated with the arrows [cf. Fig. 4(c)]. For the line scan of the filled state picture, the asymmetric shape and the width of the protrusion match very well. There is also a good agreement between the line scans of the empty state pictures [compare Figs. 5(b) and 5(c)]. Note that in both cases the two small peaks have a different height with the highest peak at the lower side of the protrusion in the filled state picture. Furthermore, comparison to the line scan of a pristine NW shows the maximum of the filled state protrusion to be located near the center of the dimer, giving the impression that the CO molecule is located on top of the NW dimer in a bridge configuration [compare Figs. 5(a) and 5(c)]. Also the location of the larger of the two small protrusions, in the empty state picture line scan, at the minimum between two NW dimers is in excellent agreement with the experimental observations [compare Figs. 5(b) and 5(c)]. This shows that a CO molecule in between two NW

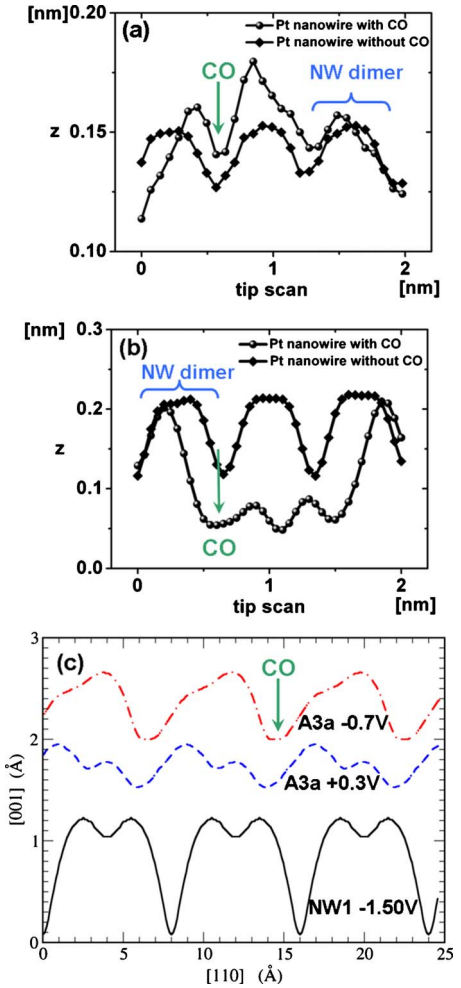

FIG. 5. (Color online) Line scans of the (a) filled- and (b) empty-state STM images of the CO adsorption site observed by Öncel *et al.* as shown in Figs. 3(a) and 3(b) (Ref. 34). A single pristine NW dimer is indicated with a curly bracket. The arrows indicate the CO location based on the calculations performed in this work. (c) Line scan images along the NW for the clean NW at a simulated bias of −1.50 V (solid black curve), the CO molecule adsorbed at the A3a site at a simulated bias of −0.70 V (dash-dotted red curve) and +0.30 V (dashed blue curve). For each system z=2.5 Å is used to generate the calculated STM images from which the line scans are taken. The lines are shifted along the [001] axis. The position of the CO molecule along the [110] axis is indicated.

dimers, bound to one NW dimer through the O atom, can look like a molecule bound on top of a NW dimer. The low binding energy found here remains problematic. However, the fact that taking into account the stretching of the molecule returns an energy comparable and better than most of the other adsorption structures indicates the energy barrier for desorption to play an important role. It also indicates that for RT experiments where a much lower CO density is present, reducing the contributions of direct and indirect interaction between CO molecules, this might not be as problematic. The good agreement of this structure with the experiment seems to support this idea and we conclude that the A3a configuration represents the geometry of the CO adsorption site observed by Öncel *et al.*

Although Öncel *et al.* do not report observing any other adsorption sites, they do report the CO molecules to perform a 1D random walk along the NW. Since the A3a adsorption site does not easily allow for a CO molecule to just jump from one site to the next, some intermediate stable adsorption sites should be present to accommodate this mobility. Looking at the geometry of the relaxed structures a path can be imagined going from A3a to A2 [cf. Fig. 1(a)], by breaking the bond between the C atom and the Pt atom at the bottom of the trough and breaking the O-Ge bond. Rotation from the A2 to the A4 configuration and onto the A1 adsorption site, followed by the same path in reverse to the next A3a site. The binding energies of these three adsorption sites (A1, A2, and A4) differs only little making it an energetically possible path at RT.[35] These sites are also present on the NW2 surface, where the adsorption site B2 can be considered an alternative for the A2 site. The calculated STM images of the B2 site also show the same asymmetric protrusion in the filled and empty state pictures, while the adsorption energy (shown in Table III) lies in the range of the three A sites. Site 3 in Fig. 3(c) clearly shows such an asymmetric adsorption site. Although the resolution in Fig. 3 is not sufficient to distinguish between the four adsorption sites mentioned above, it is sufficient to indicate their existence, and support the path for mobility proposed here.

For the NW2 surface, the calculated STM images for the adsorption sites show quite a complex picture. The simplest behavior is observed for the B4 site with the CO molecule adsorbed in a bridge configuration on a single NW dimer. Both the filled and empty state pictures show, a round, slightly asymmetric CO image sticking out far above the surface and the NW. Conversely, a CO molecule adsorbed on the B1 bridge site shows a sharp round image which becomes smaller (even invisible) for biases close to the Fermi level [cf. Figs. 6(a) and 6(b)]. A CO molecule adsorbed at the neighboring B3 site, on the other hand, shows a nice round image for negative bias [cf. filled state picture in Fig. 6(e)], which becomes a two lobed image for small positive bias but becomes invisible for large positive bias [cf. empty state picture in Fig. 6(f)].

In each of the three cases above, the CO image appears nicely centered on the NW, which can be understood from the underlying geometry. In case of a CO molecule adsorbed at the B2 site, the tilting of the molecule over the trough causes the CO image to appear only slightly shifted away from the center of the NW, giving the impression the CO molecule might be located on the wire itself [cf. Figs. 6(c) and 6(d)]. Both the filled and empty state pictures show elliptical CO images for large biases while close to the Fermi level the elliptical image becomes two lobed. As with all the previous cases where a donut or two-lobed CO image was observed, it are the π orbitals of the CO molecule that are being observed.[12]

When comparing the calculated STM images for the B1, B2, and B3 adsorption configurations shown in Fig. 6, there are a few things that need to be kept in mind. (i) The way the STM images are calculated. By using a point source as tip, almost infinitely sharp images are obtained, while in reality

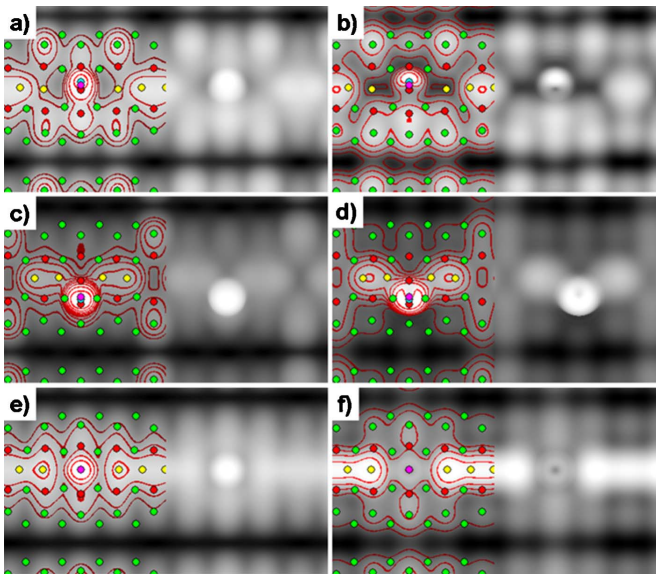

FIG. 6. (Color online) Calculated STM images of CO molecules adsorbed at the B1 [(a) and (b)], B2 [(c) and (d)], and B3 sites [(e) and (f)]. The distance above the highest atom was chosen $z = 2.0$ Å. Filled state images (a), (c), and (e) are at a simulated bias of −1.80 V while for the empty state images (d) and (f) a simulated bias of +1.80 V was used. For the empty state image (b) a simulated bias of +1.50 V was used. Contours are added to guide the eye. All contours are separated 0.2 Å in the z direction. Colored disks indicate the atom positions in the top layers. Ge and Pt atoms in the two top layers are shown in green and red, respectively. Yellow disks are used to indicate the Ge NW atoms while cyan and fuchsia is used for the C and O atoms, respectively.

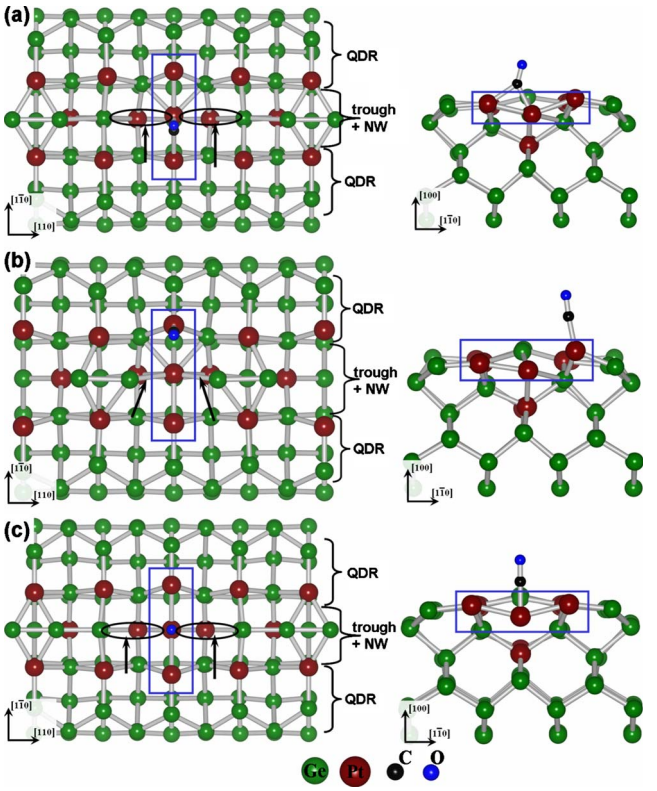

FIG. 7. (Color online) Ball-and-stick representation of a relaxed NW2 unit cell with CO molecules adsorbed at sites (a) B1, (b) B2, and (c) B3; top views are shown on the right and side views on the left. Arrows and ellipses indicate broken bonds between the Ge NW atoms and the extra Pt atom for the (a) B1 and (c) B3 adsorption sites. For the B2 adsorption site (b) these bonds, indicated with the arrows, are not broken. The QDR and the trough regions are shown for the top-view images. The three-atom monatomic Pt wire is indicated with a blue rectangle.

tip size and geometry will influence the obtained STM image. This will mainly manifest itself in a broadening of the observed features. (ii) No dynamic tip-substrate interactions are included in the calculated STM images. Although for a clean surface the effect of the tip on the surface geometry is almost negligible, this is not the case for a molecule bound to the surface.[33] At low coverage, molecules retain a large freedom to move, even if their anchor point remains fixed, resulting in a blurring of the observed STM image. (iii) The position of the molecular orbitals, especially the states above the Fermi level are not that well described in DFT (this is the well-known band-gap problem). This means that it is not always possible to use the same simulated bias as the experimental one. Points (i) and (ii) explain why the CO images in Fig. 3(c) show up to be sometimes two dimers long with a width larger than that of the NW.

With this in mind, the three adsorption sites shown in Fig. 3(c) can be identified by comparing the calculated empty and filled state pictures to experimental STM pictures. Site 1 shows a depression in the empty state picture, centered between two NW dimers. The filled state pictures on the other hand show a small protrusion.[16] Figures 6(e) and 6(f) show the same behavior for the B3 adsorbed CO molecule. Its geometry, shown in Fig. 7(c), shows the CO molecule bound in an on-top configuration to the extra Pt atom. This bond weakens the bonds between the extra Pt atom and the NW dimers, allowing the presence of the CO molecule to break them entirely, pushing the two NW dimers away from the CO molecule. The limited size of the surface cell and the periodic boundary conditions result in the formation of a Ge tetramer, and a limitation of the length of the depression to roughly 5–6 Å. However, in experiment the NW dimers could be pushed even further apart resulting in a large gap around the CO molecule, which explains the experimentally observed length of the depression to be roughly two dimer lengths. The lack of small depressions on either side of the CO molecule in the experimental filled state pictures can be understood as a consequence of the molecule-tip interactions mentioned earlier.

The second site seen in Fig. 3(c), shows a protrusion in both filled and empty state pictures. Figures 3(a) and 3(b) in Ref. 16 also show that the relative height with regard to the NW is smaller in the empty state picture than in the filled state picture. This turns out to be in agreement with the images found for the B1 adsorbed CO molecule [cf. Figs. 6(a) and 6(b)]. At this adsorption site the CO molecule is bound in a bridge configuration to the extra Pt atom and a Pt atom of the surface dimer row [cf. Fig. 7(a)]. Again the bond with the extra Pt atom allows for the bonds between the NW dimers and the extra Pt atom to be broken, and the NW

dimers to move away from the CO molecule resulting in a large gap around the CO molecule. Table III shows this bridge configuration to have the highest adsorption energy, in agreement with the *ab initio* calculations of Sclauzero *et al.*[17]

The third and last adsorption site indicated in Fig. 3(c) shows a clearly asymmetric protrusion in the empty states picture. Unfortunately no experimental filled state pictures have been published for this adsorption site but based on all the other adsorption sites observed in experiment we will assume that also in this case a protrusion is observed in the filled state image. Figures 6(c) and 6(d) show the filled and empty state pictures of a CO molecule adsorbed at site B2. This CO molecule is bound to a Pt atom in the surface dimer row, see Fig. 7(b). Because it is tilted toward the NW, the resulting image appears just slightly asymmetric of the NW, making it a very good candidate for the adsorption site 3 indicated in Fig. 3(c). In combination with the adsorption sites A1, A2, and A4, this adsorption site gives a possible migration path for the mobility observed by Öncel *et al.*[15]

In their investigation of CO adsorption on the Pt-induced NWs Kockmann *et al.* also observe a, what they call, *remarkably long-ranged repulsive interaction* between the CO molecules. This repulsion, they found, has a range up to 3–4nm (or 4–5 NW dimers) along the NW direction. Due to its long range they concluded that this repulsive interaction cannot just be a mere electrostatic repulsion. Furthermore, Kockmann *et al.* note that the characteristic long-ranged repulsive interaction is independent of the adsorption sites involved. This long-range interaction along the NW is in sharp contrast with the fact that no significant interaction is observed between CO molecules on adjacent wires. This means that the origin of the repulsive interaction needs to be linked to the NW itself. We have shown for the adsorption sites on the NW1 and the NW2 surface that the presence of CO molecules modifies the nearby NW dimers in varying degrees. When the CO molecule is located between NW dimers (e.g., A3, B1, and B3) it seems to repel the nearby NW dimers. For example, for the A3 site we find the resulting modifications to extend up to two NW dimers in each direction. Two other examples are shown in Figs. 7(a) and 7(c). They show the interaction between two periodic copies of a CO molecule on the NW2 surface. These copies are separated two NW dimers apart and can displace the neighboring NW dimers toward one-another far enough such that they form a tetramer. This effectively results in an indirect interaction between the two CO molecules. The surface strain mediating the indirect CO interaction is directed purely along the NW itself. The NW dimers which are pushed away from their original position will in their turn push further neighboring NW dimers from their equilibrium position and so on. These dislocated NW dimers block the possible adsorption sites resulting in an effective long-range repulsive interaction.

The only adsorption site left to discuss, is the B5 site. Here the CO molecule bridges the entire trough so a serious modification in the calculated STM pictures is expected. Amazingly, the calculated STM images show *nothing*. Both for filled and empty state pictures a normal NW image is observed, with not even the slightest indication of the presence of the CO molecules to be observed, making it effectively *invisible*.

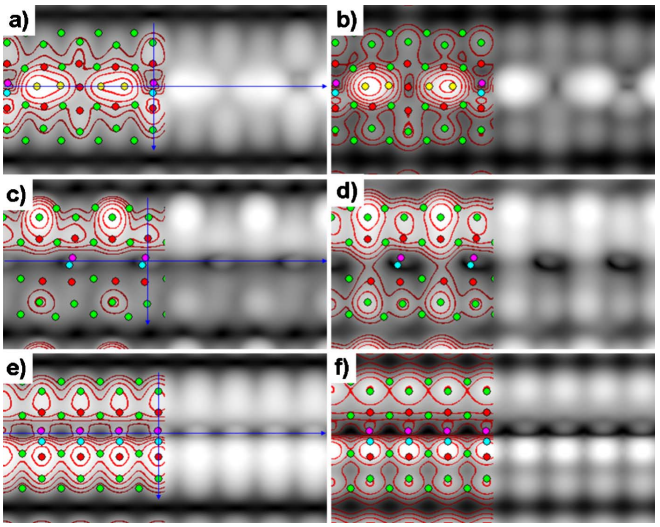

FIG. 8. (Color online) Calculated STM images of CO molecules adsorbed in bridging configurations B5 [(a) and (b)], A3b2 [(c) and (d)], and $A7_{2CO}$ [(e) and (f)]. In each case the CO molecule gives no direct image in the STM pictures, effectively remaining invisible for STM. The distance above the highest atom is chosen $z=2.0$ Å. Filled state pictures (a), (c), and (e) are at a simulated bias of −1.50 V while for the empty state pictures (b), (d), and (f) a simulated bias of +1.50 V is used. Contours are added to guide the eye and are separated 0.2 Å. Colored disks indicate the atom positions in the top layers. Ge and Pt atoms in the two top layers are shown in green and red, respectively. Yellow disks are used to indicate the Ge NW atoms while cyan and fuchsia is used for the C and O atoms, respectively. Blue arrows show the position and direction of the line scans shown in Fig. 10.

Furthermore, its high adsorption energy (only 140 meV below that of the B1 configuration) makes it also a reasonable adsorption configuration. Figures 8(a) and 8(b) show the calculated filled- and empty-state pictures. These show the CO molecule to be invisible while the rest of the NW image remains unchanged. This is also the case for other simulated biases (±0.30 and ±0.70 eV), leading to the conclusion that this adsorption configuration could well be present in experiment but invisible for STM. Only high-resolution line scans orthogonal to the NWs at the position indicated in Fig. 8(a) could show the induced asymmetry of the QDRs [cf. Fig. 10], possibly combined with the observation that these asymmetric line scans are on average lower than those symmetric ones on locations where no CO molecule is present. Another way one could imagine to make the CO molecule appear, is by breaking its O-Pt bond with a small current surge through the STM tip. After breaking this bond, the CO molecule might then revert to the B2 adsorption configuration, which is clearly visible in both filled and empty state pictures [cf. Figs. 6(c) and 6(d)].

This is for the case where the substrate is a NW array. For solitary NWs, which we have already shown to be less stable under CO adsorption, observation of a B5 configuration (referred to as A7 on the NW1 substrate) would be easier. The steric repulsion between the CO molecule and the NW dimers will create a hole in the NW centered around the CO molecule. This defect should show up over a wide range of

TABLE IV. Formation and adsorption energies for CO adsorbed in configurations bridging the trough between two neighboring QDRs. Adsorption sites are shown in Fig. 9(a). The B5 and A3b values are duplicated from Table I for ease of comparison. $\mathbf{r}_{CO}$, $\mathbf{r}_{C\text{-surf}}$, and $\mathbf{r}_{O\text{-Pt}}$ are the C-O, C-Pt, and O-Pt bond lengths, the value between brackets for $\mathbf{r}_{C\text{-surf}}$ is the bond length of the C atom to the Pt atom at the bottom of the trough. $\mathbf{a}_{CO}$ and $\mathbf{a}_{C\text{-surf}}$ are the bond angles with regard to the surface plane. In case of bridge adsorption $\mathbf{a}_{C\text{-surf}}$ is the angle between the two C-surface bonds.

	E_f (eV)	E_{ad} (eV)	Coord.	$\mathbf{r}_{CO}$ (Å)	$\mathbf{a}_{CO}$ (deg)	$\mathbf{r}_{C\text{-surf}}$ (Å)	$\mathbf{a}_{C\text{-surf}}$ (deg)	$\mathbf{r}_{O\text{-Pt}}$ (Å)
NW1 A3b	−1.485	−2.069	b	1.214	47	2.012(2.066)	101	2.249
NW1 A3b1	−1.163	−2.276	b	1.207	43	1.960(2.106)	90	2.167
NW1 A3b2	0.390	−2.094	b	1.204	44	1.964(2.084)	87	2.190
NW2 B5	−0.784	−2.197	t	1.170	20	1.883	28	2.433
NW1 A7	−1.589	−2.361	t	1.169	17	1.884	28	2.401
NW1 $A7_{2CO}$	−3.741	−2.214	t	1.167	19	1.882	27	2.394

biases as a depression containing a small protrusion in its center and a width of at least 8 Å.[36] Table IV shows the A7 configuration [cf. Fig. 9(b)] to have a very high adsorption energy, leading to the assumption that this configuration should also be observed in experiments.

B. Molecular electronics on Pt modified Ge(001)?

From these calculations and the experiments presented in literature, the possible application of this system for 1D molecular electronics becomes very unlikely. The long-ranged interaction observed by Kockmann *et al.* and its explanation in light of the calculations performed in this work, seems to be the main problem.

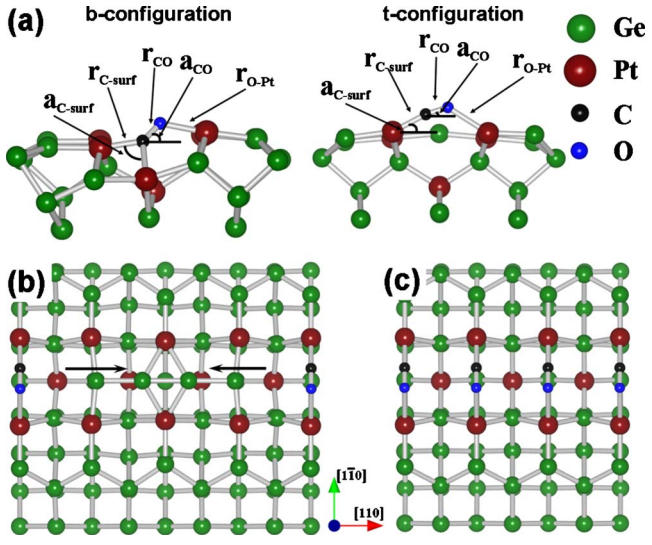

FIG. 9. (Color online) (a) Ball-and-stick representation of the two types of bridging CO configurations. In case of a t(op) configuration the C atom is bound to a single substrate atom while in a b(ridge) configuration the C atom is bound to two substrate atoms. Geometrical parameters given in Table IV are indicated, where values for different CO densities and substrates are presented. (b) and (c) show ball-and-stick representation of two systems with a t configuration and different CO density: (b) the A7 and (c) $A7_{2CO}$ structures. Arrows in (b) show the drift direction of the NW dimers.

Up to this point we focused on identifying the experimentally observed structures. The B5 adsorption configuration and the comparable A3b configuration have not yet been discussed in light of experiments while showing almost the best adsorption energies. The calculated STM images for these structures show something very peculiar: the total lack of an image for the CO molecule. In case of the A3b adsorption site a large protrusion is still visible, however this is an ejected Ge atom of the NW dimer [cf. Fig. 2(b)]. This ejection was due to the limited unit-cell size. The steric repulsion between two periodic copies of the CO molecule and the single Ge NW dimer prohibited the Ge dimer to be displaced sufficiently along the NW direction. To remove this "computational artifact" the ejected Ge atom is removed (A3b1) and in a second calculation both Ge atoms forming the NW dimer are removed (A3b2). Also an adsorption structure with B5 configuration on a NW1 surface is build (A7), using a double NW1 surface cell. Table IV shows the formation and adsorption energies for these new structures in comparison to the B5 and A3b structures. Removal of the Ge NW atoms clearly decreases the formation energy of the surface, which is due to the uncovering of the imbedded Pt atoms.[19] The adsorption energy of the CO molecule however remains roughly the same. Also the geometrical parameters barely change. The bond lengths decrease slightly, owing to the reduced steric repulsion between the CO molecules and the Ge dimer atoms, moving the CO molecule closer to the surface.

In case of the A7 adsorption configuration, the lack of anchor point for the NW dimers causes them to drift away from the CO molecule due to the steric repulsion. Which, because of the limited unit cell size, results in the formation of a Ge tetramer as is shown in Fig. 9(b). The geometric parameters for the CO molecules in the B5 and A7 adsorption configurations are almost identical. However, the distance between a CO molecule and the nearest Ge atom of a NW dimer is approximately 4.3 Å in case of the A7 configuration while it is only 3.3 Å in case of the B5 configuration. This shows the improvement in adsorption energy, going from the B5 to the A7 configuration, can be attributed to the reduction in the steric repulsion between the CO molecule and the Ge NW dimers.

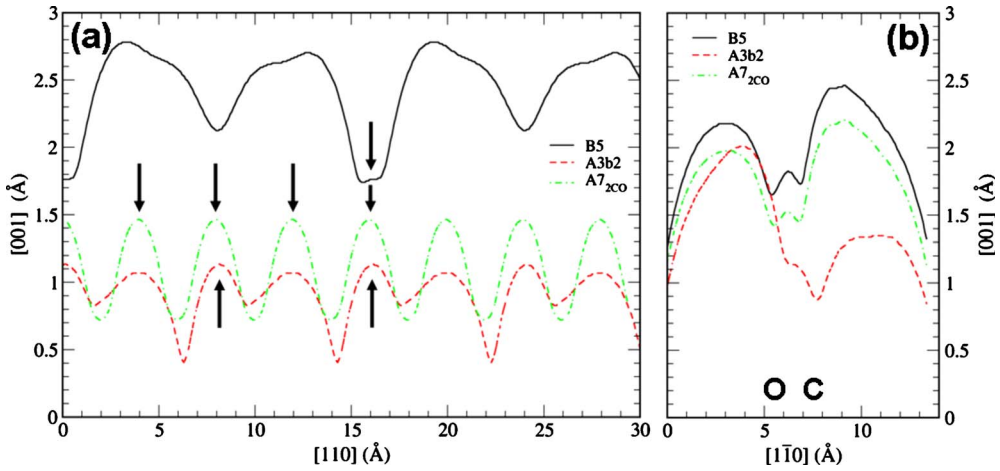

FIG. 10. (Color online) Calculated (a) line scan images along and (b) orthogonal to the trough/NW for the B5 (solid black curve), the A3b2 (red dashed curve), and the A7$_{2CO}$ (green dash-dot curve) configuration. The line scans are taken along the arrows shown in Figs. 8(a), 8(c), and 8(e). The arrows in (a) indicate the positions of the CO molecules while C and O show the positions of the C and O atom in (b).

Because uncovering the imbedded Pt atoms has a negative influence on the formation energy, a model is build with the entire NW removed and replaced by a maximum coverage of CO molecules in an A7 configuration (A7$_{2CO}$). The A7$_{2CO}$ structure contains two CO molecules per 4×2 surface cell [cf. Fig. 9(c)], making this a four times higher coverage than the A7 case. A large increase in the formation energy is found while the steric repulsion only has a minute influence on the adsorption energy of the CO molecules. Furthermore, the geometrical parameters remain almost unchanged making this, from the geometrical point of view, a very good candidate for 1D molecular electronics. However, one small problem remains: these CO molecules in either b or t bridging configuration are invisible in STM. Figure 8 shows both filled and empty state pictures of the B5, A2b2, and A7$_{2CO}$ adsorption geometries. For the B5 adsorption configuration the line scan (black solid line shown in Fig. 10) is almost unmodified compared to the line scan of the pristine NW. The only modification is found in the line scan orthogonal to the trough/NW. In case of a t bridging configuration, the dimer of the QDR which is bound to the C atom is higher than the dimer bound to the O atom while the opposite is true for the b bridging configuration.

In conclusion, if one would succeed in stripping away the Ge NW without damaging the underlying substrate, a high coverage of CO molecules in bridging configuration could be recognized by this asymmetry in the QDR images. The formation and adsorption energies are highly favorable, making this also energetically an interesting template for 1D molecular electronics.

V. CONCLUSIONS

In this paper we studied the adsorption of CO molecules on Pt-induced NWs on Ge(001) using *ab initio* DFT calculations. We show that CO has a strong preference for adsorption on the Pt atoms imbedded in the Ge(001) surface. As a consequence CO molecules do not bind directly on top of the Ge dimers forming the NWs, contrary to the experimental assumptions. By direct comparison of calculated STM images to experimental STM images we have successfully identified the observed adsorption sites. We have shown that the Pt atoms lining the troughs in which the Ge NWs are imbedded provide the necessary adsorption sites to explain all experimentally observed CO adsorption sites.

CO molecules in on-top configurations next to the NW tilt toward it, presenting STM images located "on" the NW. CO molecules bound in between NW dimers with the O atom also bound to a Ge NW dimer atom (A3a configuration) modify the electronic structure of this Ge atom sufficiently to give the appearance of a protrusion on the Ge dimer. This gives rise to the short-bridge CO adsorption site observed by Öncel *et al.* A CO molecule bound in an on-top configuration on the extra Pt atom of the NW2 surface, showing a protrusion at negative bias and a depression at positive bias (B3 configuration), is found to show good agreement with the experimentally observed long-bridge site, seen by Kockmann *et al.* The short-bridge site observed by this group is identified as a CO molecule in a bridge configuration in between NW dimers (B1 configuration).

A path for mobility along the wire is presented, showing the CO molecule to move along the Pt atoms of the underlying QDRs (A3$\rightarrow$A2/B2$\rightarrow$A4$\rightarrow$A1 and back). The long-ranged interaction observed by Kockmann *et al.* is explained trough the dislocation of NW dimers, in the vicinity of the CO molecule. These dislocated NW dimers in turn block the nearby CO adsorption sites.

We also predict the presence of bridging CO molecules invisible in standard STM experiments, and present methods for observing them experimentally. Also the possibility of 1D molecular electronics is touched. After removal of the Ge NW dimers, stable, invisible wires of parallel CO molecules, along the Pt lined troughs, can be obtained. This configuration has a large formation energy $E_f=-3.74$ eV and an adsorption energy per CO molecule $E_{ad}=-2.21$ eV at maximum CO coverage.

ACKNOWLEDGMENTS

We thank Harold Zandvliet for the interesting discussions

and Nuri Öncel and Daan Kockmann for making their experimental data available. This work is part of the research program of the "Stichting voor Fundamenteel Onderzoek der Materie" (FOM) and the use of supercomputer facilities was sponsored by the "Stichting Nationale Computer Faciliteiten" (NCF), both financially supported by the "Nederlandse Organisatie voor Wetenschappelijk Onderzoek" (NWO).

*Present address: Department of Inorganic and Physical Chemistry, Ghent University, Krijgslaan 281-S3, 9000 Gent, Belgium; dannyvanpoucke@gmail.com; http://users.ugent.be/~devpouck/

[1] A. Eichler, Surf. Sci. **498**, 314 (2002).
[2] R. Imbihl and G. Ertl, Chem. Rev. **95**, 697 (1995).
[3] G. Ertl, M. Neumann, and K. M. Streit, Surf. Sci. **64**, 393 (1977).
[4] H. Froitzheim, H. Hopster, H. Ibach, and S. Lehwald, Appl. Phys. (Berlin) **13**, 147 (1977).
[5] H. Steininger, S. Lehwald, and H. Ibach, Surf. Sci. **123**, 264 (1982).
[6] D. F. Ogletree, M. A. V. Hove, and G. A. Somorjai, Surf. Sci. **173**, 351 (1986).
[7] Y. Y. Yeo, L. Vattuone, and D. A. King, J. Phys. Chem. **106**, 392 (1997).
[8] P. J. Feibelman, B. Hammer, J. K. Norskov, F. Wagner, M. Scheffler, R. Stumpf, R. Watwe, and J. Dumesic, J. Phys. Chem. B **105**, 4018 (2001), and references herein.
[9] P. van Beurden, H. G. J. Verhoeven, G. J. Kramer, and B. J. Thijsse, Phys. Rev. B **66**, 235409 (2002).
[10] M. Alaei, H. Akbarzadeh, H. Gholizadeh, and S. de Gironcoli, Phys. Rev. B **77**, 085414 (2008).
[11] I. Dabo, A. Wieckowski, and N. Marzari, J. Am. Chem. Soc. **129**, 11045 (2007).
[12] M. L. Bocquet and P. Sautet, Surf. Sci. **360**, 128 (1996).
[13] M. Ø. Pedersen, M.-L. Bocquet, P. Sautet, E. Lægsgaard, I. Stensgaard, and F. Besenbacher, Chem. Phys. Lett. **299**, 403 (1999).
[14] O. Gurlu, O. A. O. Adam, H. J. W. Zandvliet, and B. Poelsema, Appl. Phys. Lett. **83**, 4610 (2003).
[15] N. Öncel, W. J. van Beek, J. Huijben, B. Poelsema, and H. J. W. Zandvliet, Surf. Sci. **600**, 4690 (2006).
[16] D. Kockmann, B. Poelsema, and H. J. W. Zandvliet, Phys. Rev. B **78**, 245421 (2008).
[17] G. Sclauzero, A. Dal Corso, A. Smogunov, and E. Tosatti, Phys. Rev. B **78**, 085421 (2008).
[18] D. E. P. Vanpoucke and G. Brocks, Phys. Rev. B **77**, 241308 (2008).
[19] D. E. P. Vanpoucke and G. Brocks, Phys. Rev. B **81**, 085410 (2010).
[20] K. Fukutani, T. T. Magkoev, Y. Murata, M. Matsumoto, T. Kawauchi, T. Magome, Y. Tezuka, and S. Shin, J. Electron Spectrosc. Relat. Phenom. **88-91**, 597 (1998).
[21] D. E. P. Vanpoucke and G. Brocks, Mater. Res. Soc. Symp. Proc. **1177E**, 1177-Z03-09 (2009).
[22] P. E. Blöchl, Phys. Rev. B **50**, 17953 (1994).
[23] G. Kresse and D. Joubert, Phys. Rev. B **59**, 1758 (1999).
[24] G. Kresse and J. Hafner, Phys. Rev. B **47**, 558 (1993).
[25] G. Kresse and J. Furthmüller, Phys. Rev. B **54**, 11169 (1996).
[26] H. J. Monkhorst and J. D. Pack, Phys. Rev. B **13**, 5188 (1976).
[27] J. Tersoff and D. R. Hamann, Phys. Rev. B **31**, 805 (1985).
[28] The NW at the edge of a NW array next to bare β terrace, just like a solitary NW, does not present the 4×1 periodicity typical for NWs in a NW array. It was argued in Ref. 19 that these edge NWs might have the same geometry as the solitary NWs. The latter could be understood to be an extreme case of a NW array, i.e., one only consisting of its edge. Because of this, we will refer to both solitary and edge NWs as solitary NWs while array NWs refers to the none-edge NWs of a NW array.
[29] A. van Houselt, T. Gnielka, J. M. J. Aan de Brugh, N. Öncel, D. Kockmann, R. Heid, K. P. Bohnen, B. Poelsema, and H. Zandvliet, Surf. Sci. **602**, 1731 (2008).
[30] O. R. Gilliam, C. M. Johnson, and W. Gordy, Phys. Rev. **78**, 140 (1950).
[31] R. Hirschl, F. Delbecq, P. Sautet, and J. Hafner, Phys. Rev. B **66**, 155438 (2002).
[32] Two surface unit cells are shown in Fig. 2(b).
[33] M. M. D. Ramos, A. P. Sutton, and A. M. Stoneham, J. Phys.: Condens. Matter **3**, S127 (1991).
[34] N. Öncel, Ph.D. thesis, University of Twente, 2007.
[35] The computational cost to calculate diffusion barriers between these intermediate steps is, due to the system size, too large, so no diffusion barriers were calculated.
[36] In our limited surface cell the NW dimers could not spread further before colliding with periodic copies, limiting the width of the depression to ~8 Å.